Measurement of Subpicosecond Time Intervals between Two Photons by Interference

C. K. Hong, Z. Y. Ou, and L. Mandel

Department of Physics and Astronomy, University of Rochester, Rochester, New York 14627

A fourth-order interference technique has been used to measure the time intervals between two photons, and by implication the length of the photon wave packet, produced in the process of parametric down-conversion. The width of the time-interval distribution, which is largely determined by an interference filter, is found to be about 100 fs, with an accuracy that could, in principle, be less than 1 fs.

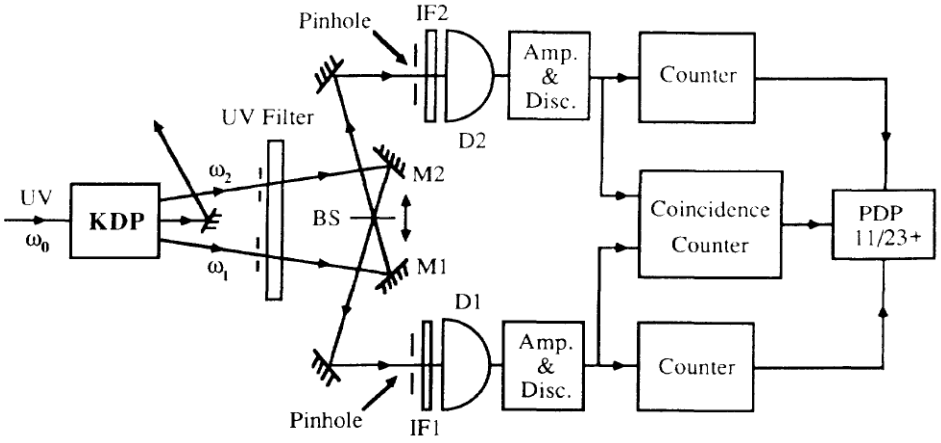

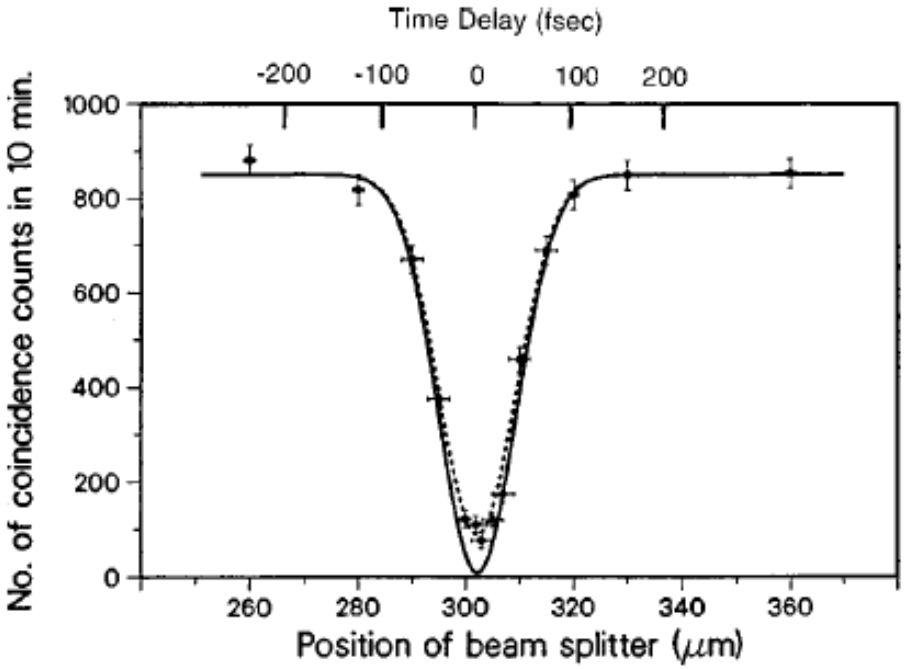

FIG. 2. The measured number of coincidences as a function of beam-splitter displacement $c\,\delta\tau$, superimposed on the solid theoretical curve derived from Eq. (11) with $R/T=0.95$, $\Delta\omega=3\times10^{13}$ rad s^{-1}. For the dashed curve the factor $2RT/(R^2+T^2)$ in Eq. (11) was multiplied by 0.9. The vertical error bars correspond to one standard deviation, whereas horizontal error bars are based on estimates of the measurement accuracy.

Observation of Nonclassical Effects in the Interference of Two Photons

R. Ghosh and L. Mandel

Department of Physics and Astronomy, University of Rochester, Rochester, New York 14627

(Received 21 May 1987)

By measuring the joint probability for the detection of two photons at two points as a function of the separation between the points, we have demonstrated the existence of nonclassical effects in the interference of signal and idler photons in parametric down-conversion. In principle, the detection of one photon at one point rules out certain positions where the other photon can appear.

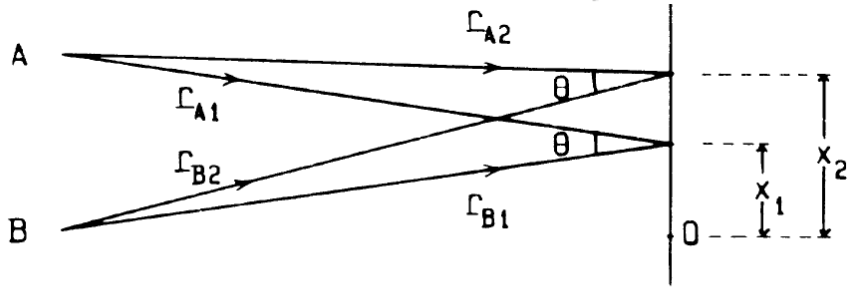

FIG. 1. The geometry of the interference experiment.

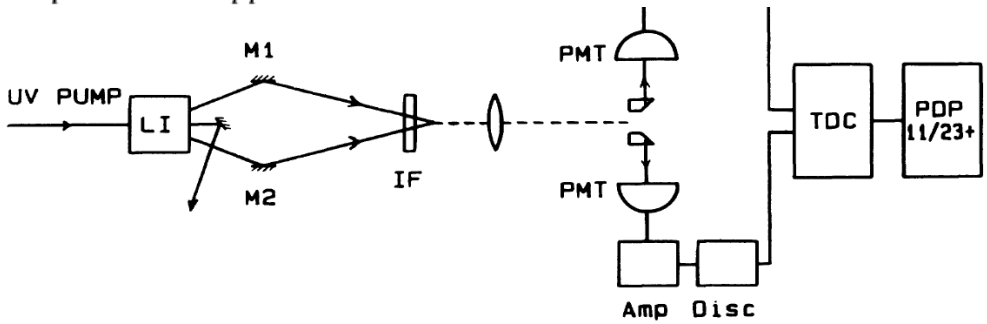

FIG. 2. Outline of the apparatus.

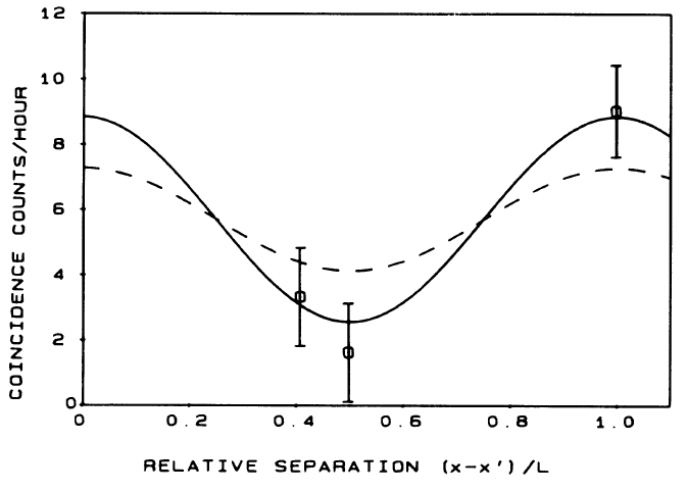

FIG. 3. Experimental results superimposed on the predictions of quantum theory given by Eq. (9) (full curve), and of the classical theory with maximum modulation (dashed curve).

Evidence for phase memory in two-photon down conversion through entanglement with the vacuum

Z. Y. Ou, L. J. Wang, X. Y. Zou, and L. Mandel
Department of Physics and Astronomy, University of Rochester, Rochester, New York 14627
(Received 14 August 1989)

An experiment has been carried out in which two pairs of light beams produced by down conversion in two nonlinear crystals driven by a common pump were mixed by two beam splitters, and the coincidence rate for simultaneous detections of mixed signal and idler photons was measured. It is found that the down-converted light carries information about the phase of the pump field through the entanglement of the down-converted photons with the vacuum.

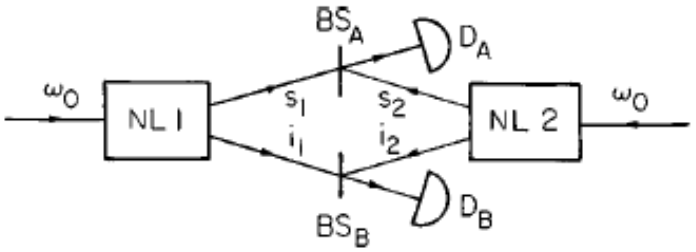

FIG. 3. Principle of the interference experiment with two downconverters in which both one-photon and two-photon interference can be investigated (after Ou *et al.*, 1990).

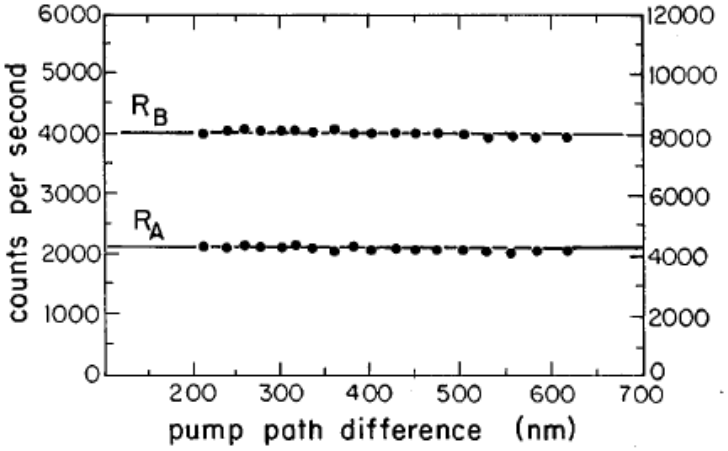

FIG. 4. Results of measurements of the photon counting rate by D_A and D_B in Fig. 3 as a function of path difference, showing the absence of one-photon interference.

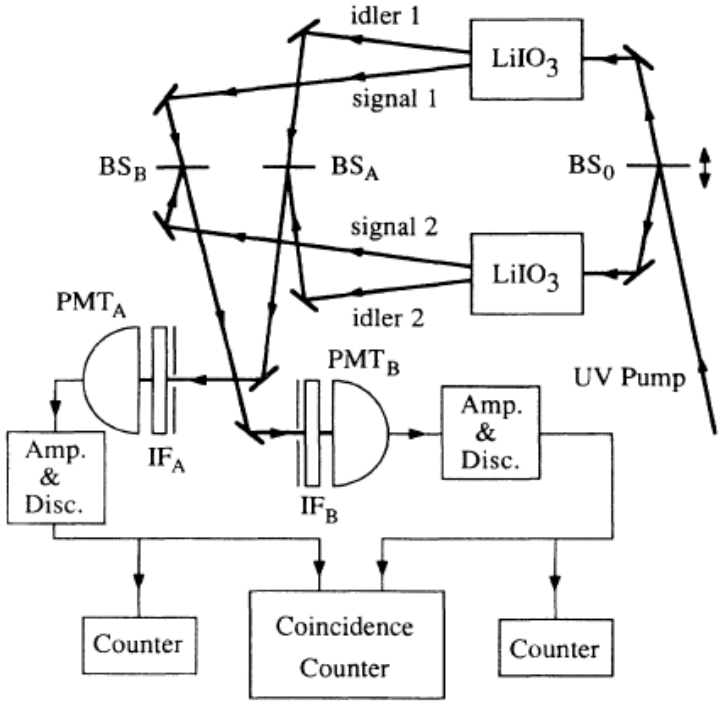

FIG. 2. The setup used in the experiment.

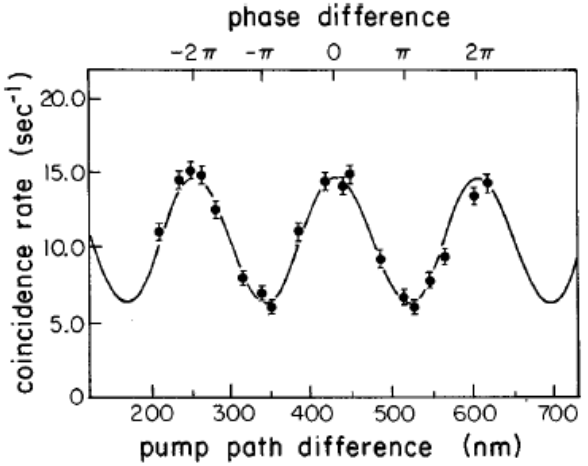

FIG. 5. Results of coincidence measurements by D_A and D_B in Fig. 3 as a function of path difference, showing two-photon interference. The continuous curve is theoretical.

Induced Coherence and Indistinguishability in Optical Interference

X. Y. Zou, L. J. Wang, and L. Mandel

Department of Physics and Astronomy, University of Rochester, Rochester, New York 14627

(Received 18 March 1991)

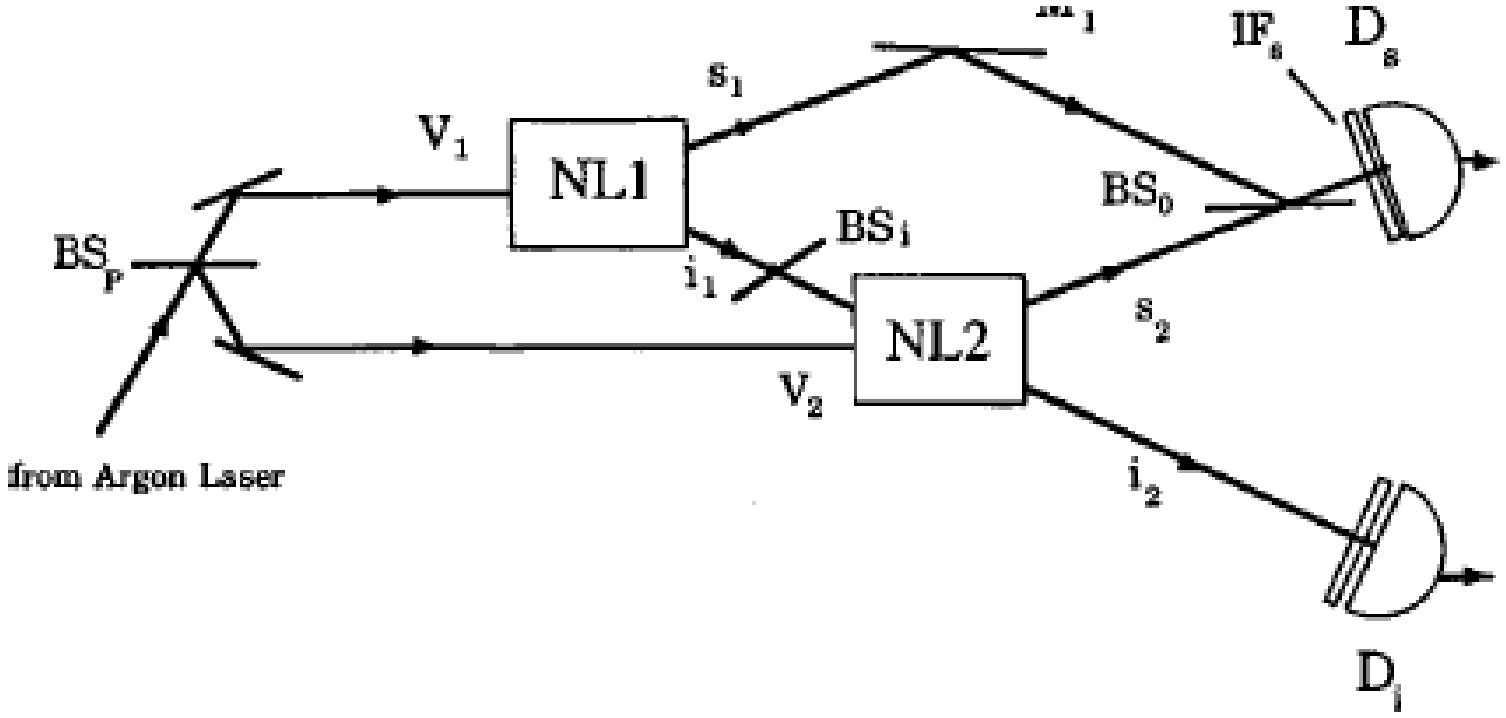

Induced Coherence and Indistinguishability in Optical Interference

X. Y. Zou, L. J. Wang, and L. Mandel

Department of Physics and Astronomy, University of Rochester, Rochester, New York 14627

(Received 18 March 1991)

Second-order interference is observed in the superposition of signal photons from two coherently pumped parametric down-converters, when the paths of the idler photons are aligned. The interference exhibits certain nonclassical features; it disappears when the idlers are misaligned or separated by a beam stop. The interpretation of this effect is discussed in terms of the intrinsic indistinguishability of the photon paths.

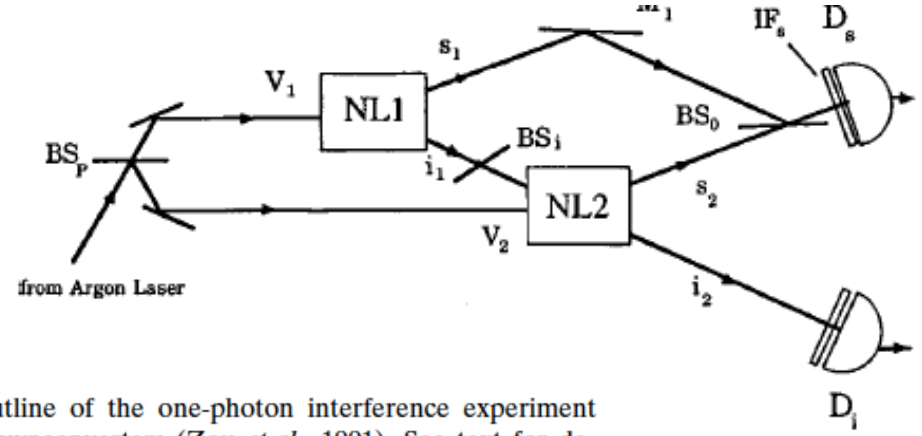

FIG. 6. Outline of the one-photon interference experiment with two downconverters (Zou *et al.*, 1991). See text for description.

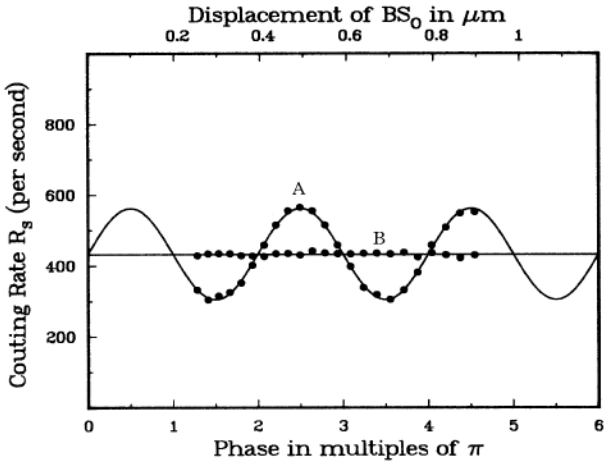

FIG. 2. Measured photon counting rate R_s as a function of beam-splitter BS$_O$ displacement. Curve *A*: neutral-density filter with $|\mathcal{T}|=0.91$ between NL1 and NL2; curve *B*: beam stop with $\mathcal{T}=0$ inserted between NL1 and NL2. 1 standard deviation is smaller than the dot size. The solid curves are the best-fitting sinusoidal functions of period 394 nm.

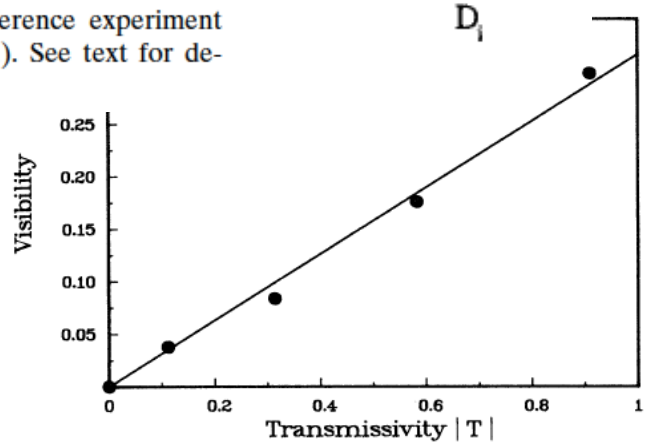

FIG. 3. Measured visibility $\mathcal{V}$ of the second-order interference pattern as a function of amplitude transmissivity $|\mathcal{T}|$ of the filter placed between NL1 and NL2. The uncertainties are comparable with or smaller than the dot size.

Propagation of transient quantum coherence

L. J. Wang and J.-K. Rhee
NEC Research Institute, Inc., 4 Independence Way, Princeton, New Jersey 08540
(Received 23 January 1998; revised manuscript received 18 August 1998)

We perform a time-resolved quantum interference experiment based on the effect of induced coherence without induced emission using two pulsed parametric down-conversion sources. We periodically vary the transmission of the first source's idler beam and measure the time-dependent visibility of fringes in the interference between the two signal beams. The visibility is found to be correlated with the transmissivity with a time delay corresponding to a combined path of the first idler and the second signal beam. The experiment is discussed in the context of the delayed choice experiments. [S1050-2947(99)09402-0]

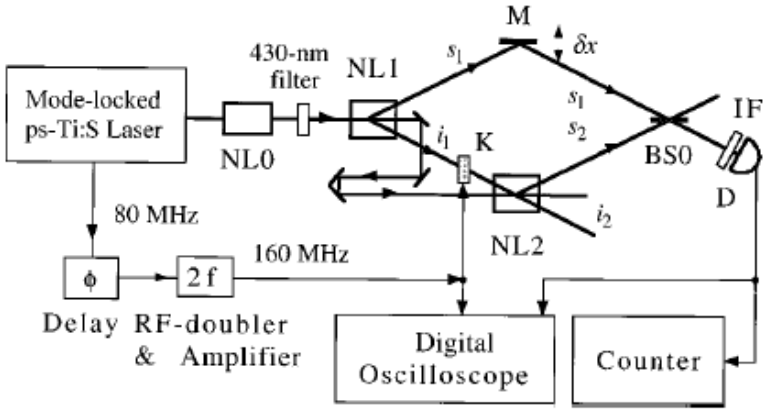

FIG. 1. Schematic setup of the experiment.

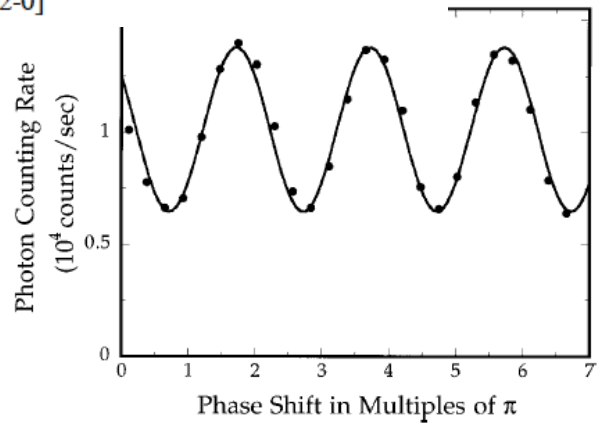

FIG. 2. Typical interference pattern recorded with the avalanche photodiode, *D*. The optical phase shift is introduced by moving the mirror *M*. One standard deviation is smaller than the dot size. The solid curve is the least-squares-fitting sinusoidal of period 860 nm.

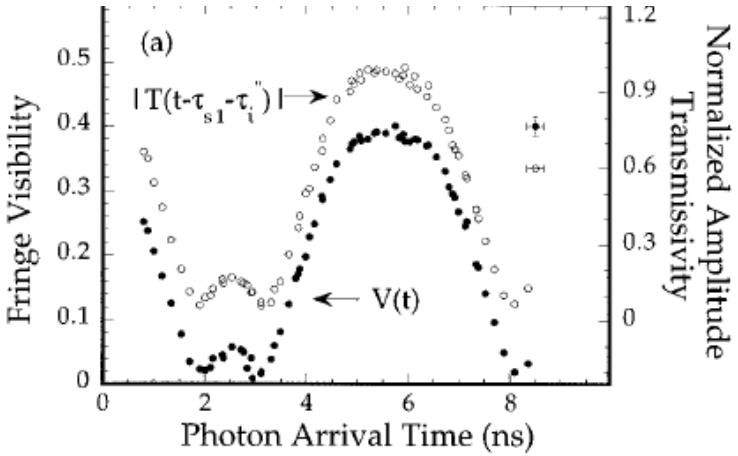

FIG. 3. (a) Time-dependent fringe visibility and the EO modulator's amplitude tramsmissivity. Here the horizontal axis is time relative to the 160 MHz signal that drives the EO modulator. The visibility $V(t)$ (dots) is extracted from the fringes exhibited by photons arriving at the detector at time t. The EO's amplitude transmissivity at an earlier time $(t-\tau_{s2}-\tau_i'')$ is also shown (open circles). Error bars on the right corner represent one standard deviation. (b) Fringe visibility $V(t)$ vs the amplitude transmissivity $|T(t-\tau_{s2}-\tau_i'')|$. The straight line is the least-squares fit.

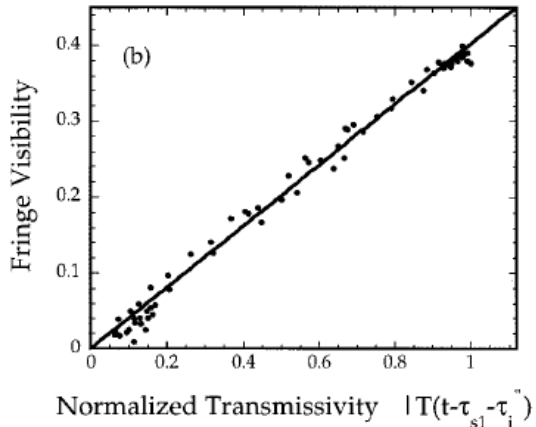

Measurement of the Photonic de Broglie Wavelength of Entangled Photon Pairs Generated by Spontaneous Parametric Down-Conversion

Keiichi Edamatsu, Ryosuke Shimizu, and Tadashi Itoh

Division of Materials Physics, Graduate School of Engineering Science, Osaka University, Toyonaka 560-8531, Japan

(Received 21 February 2002; published 4 November 2002)

Using a basic Mach-Zehnder interferometer, we demonstrate experimentally the measurement of the photonic de Broglie wavelength of entangled photon pairs (biphotons) generated by spontaneous parametric down-conversion. The observed interference manifests the concept of the photonic de Broglie wavelength. We also discuss the phase uncertainty obtained from the experiment.

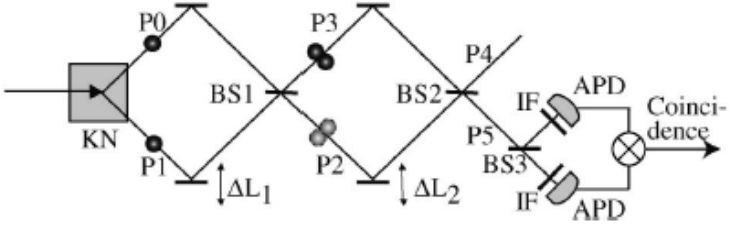

FIG. 1. Schematic experimental setup of the biphoton interference. KN: $KNbO_3$ crystal, BS1 ~ 3: beam splitters, IF: interference filters, APD: avalanche photodiodes.

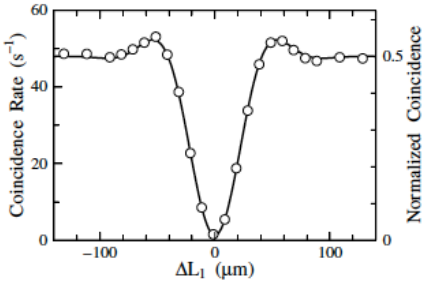

FIG. 2. Coincidence-photon-counting rate detected at the two output ports of BS1 as a function of the optical path-length difference (ΔL_1) between the two paths from KN and BS1 in Fig. 1. Open circles indicate experimental data, and the solid curve is a fitted function that assumes the observed photons have a rectangular spectral shape.

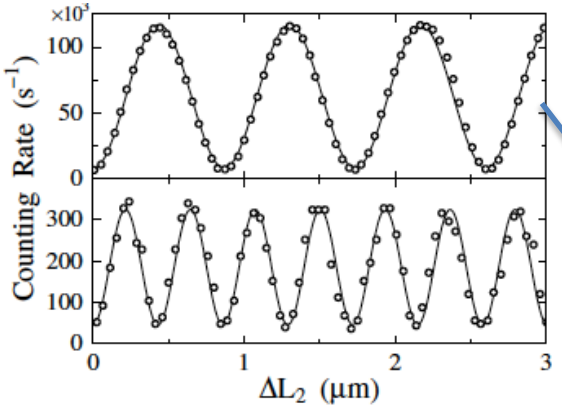

FIG. 3. Interference patterns in the one-photon (upper) and two-photon (lower) counting rates at a path-length difference of around 0 μm.

Block P1 (only 1 photon input)

{No single-photon interference with |1,1> input.}

Optical-Fiber Source of Polarization-Entangled Photons in the 1550 nm Telecom Band

Xiaoying Li,* Paul L. Voss, Jay E. Sharping, and Prem Kumar

Center for Photonic Communication and Computing, ECE Department, Northwestern University, Evanston, Illinois 60208-3118, USA

(Received 12 August 2004; published 9 February 2005)

We present a fiber-based source of polarization-entangled photons that is well suited for quantum communication applications in the 1550 nm band of standard fiber-optic telecommunications. Polarization entanglement is created by pumping a nonlinear-fiber Sagnac interferometer with two time-delayed orthogonally polarized pump pulses and subsequently removing the time distinguishability by passing the parametrically scattered signal and idler photon pairs through a piece of birefringent fiber. Coincidence detection of the signal and idler photons yields biphoton interference with visibility greater than 90%, while no interference is observed in direct detection of either signal or idler photons. All four Bell states can be prepared with our setup and we demonstrate violations of the Clauser-Horne-Shimony-Holt form of Bell's inequality by up to 10 standard deviations of measurement uncertainty.

Tailored Photon-Pair Generation in Optical Fibers

Offir Cohen,* Jeff S. Lundeen, Brian J. Smith, Graciana Puentes, Peter J. Mosley, and Ian A. Walmsley

Clarendon Laboratory, University of Oxford, Parks Road, Oxford, OX1 3PU, United Kingdom

(Received 29 August 2008; published 27 March 2009)

We experimentally control the spectral structure of photon pairs created via spontaneous four-wave mixing in microstructured fibers. By fabricating fibers with designed dispersion, one can manipulate the photons' wavelengths, joint spectrum, and, thus, entanglement. As an example, we produce photon pairs with no spectral correlations, allowing direct heralding of single photons in pure-state wave packets without filtering. We achieve an experimental purity of (85.9 ± 1.6)%, while theoretical analysis and preliminary tests suggest that 94.5% purity is possible with a much longer fiber.

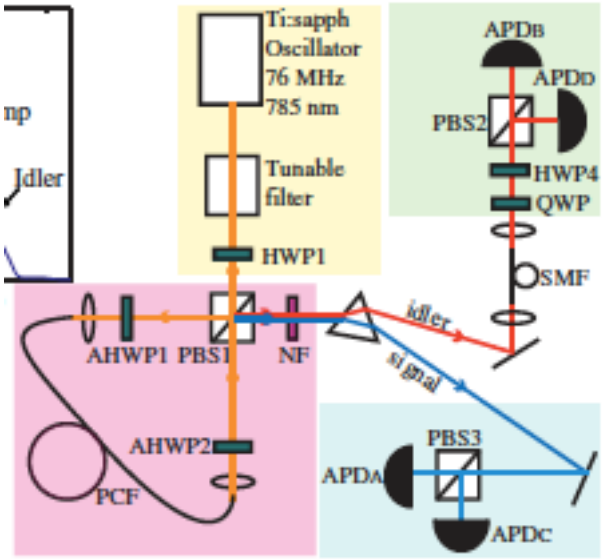

FIG. 2 (color online). Fiber spectrum (inset) and polarization HOM experimental setup. Although some Raman background remains at the idler wavelength, the lack of background at the signal ensures that coincidence detection events most likely originate from SFWM.

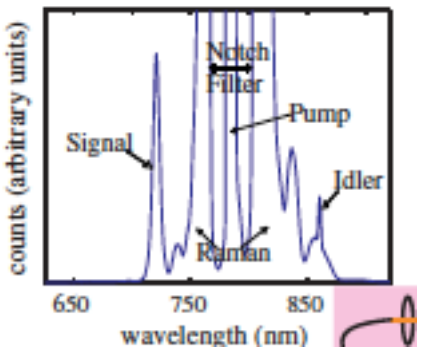

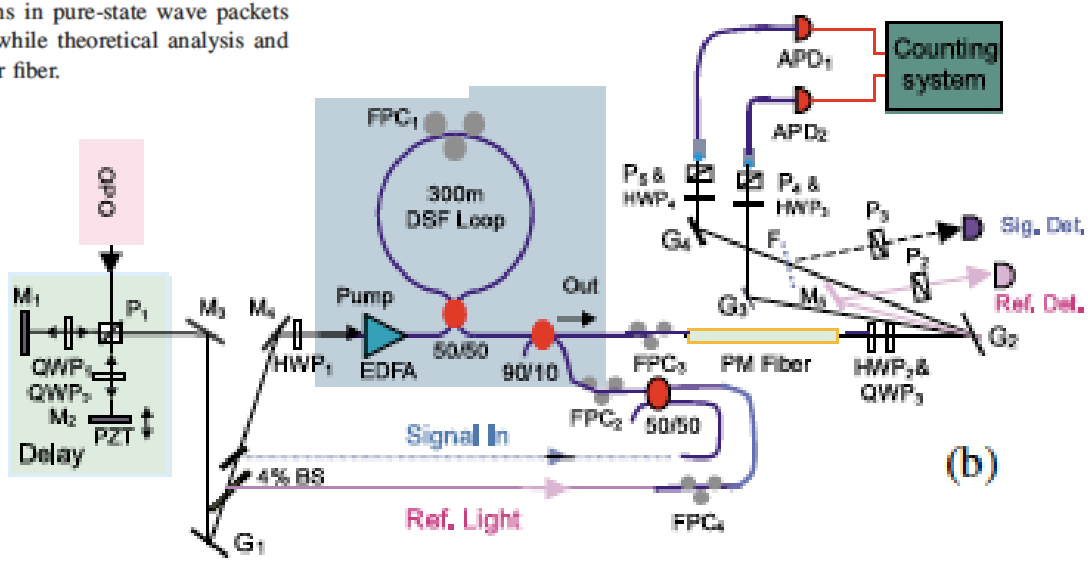

Narrow Band Source of Transform-Limited Photon Pairs via Four-Wave Mixing in a Cold Atomic Ensemble

Bharath Srivathsan,[1] Gurpreet Kaur Gulati,[1] Brenda Chng,[1] Gleb Maslennikov,[1] Dzmitry Matsukevich,[1,2] and Christian Kurtsiefer[1,2,*]

[1]*Centre for Quantum Technologies, National University of Singapore, 3 Science Drive 2, Singapore 117543, Singapore*
[2]*Department of Physics, National University of Singapore, 2 Science Drive 3, Singapore 117542, Singapore*

(Received 15 February 2013; published 17 September 2013)

We observe narrow band pairs of time-correlated photons of wavelengths 776 and 795 nm from nondegenerate four-wave mixing in a laser-cooled atomic ensemble of ^{87}Rb using a cascade decay scheme. Coupling the photon pairs into single mode fibers, we observe an instantaneous rate of 7700 pairs per second with silicon avalanche photodetectors, and an optical bandwidth below 30 MHz. Detection events exhibit a strong correlation in time [$g^{(2)}(\tau = 0) \approx 5800$] and a high coupling efficiency indicated by a pair-to-single ratio of 23%. The violation of the Cauchy-Schwarz inequality by a factor of 8.4×10^6 indicates a strong nonclassical correlation between the generated fields, while a Hanbury Brown–Twiss experiment in the individual photons reveals their thermal nature. The comparison between the measured frequency bandwidth and $1/e$ decay time of $g^{(2)}$ indicates a transform-limited spectrum of the photon pairs. The narrow bandwidth and brightness of our source makes it ideal for interacting with atomic ensembles in quantum communication protocols.

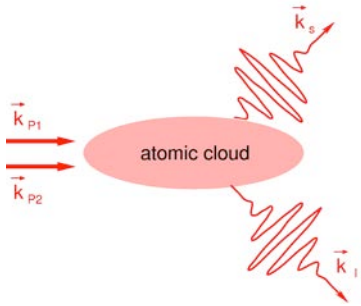

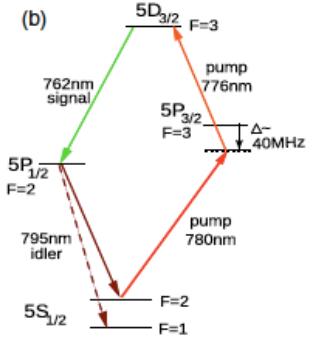

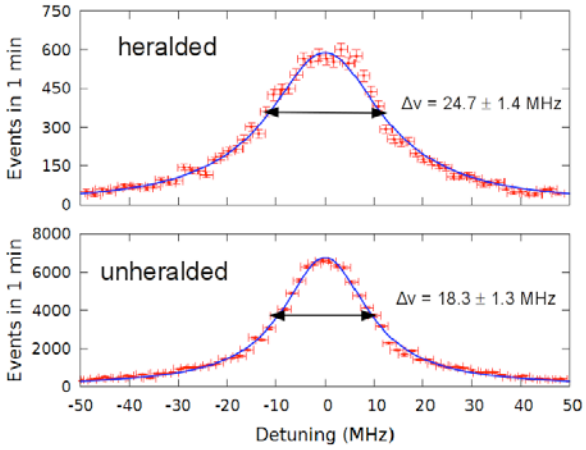

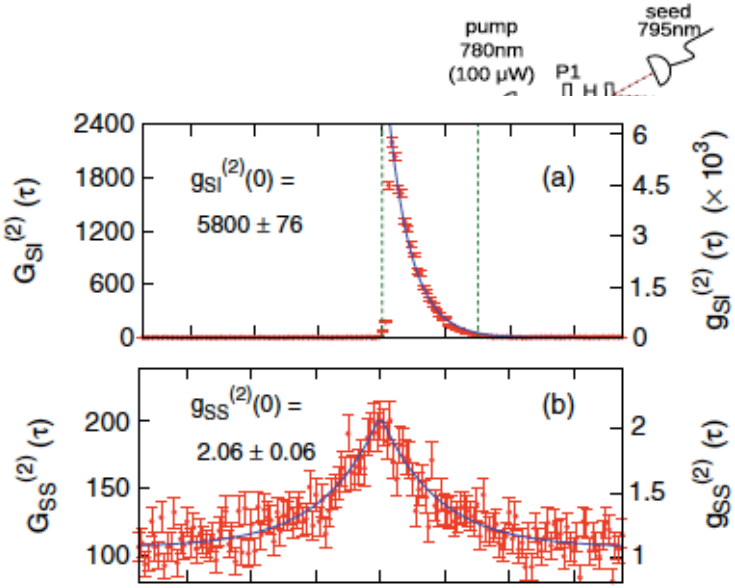

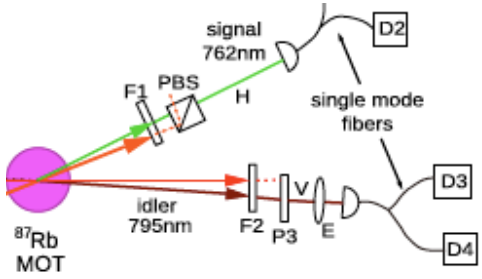

Mechanical Detection and Measurement of the Angular Momentum of Light

RICHARD A. BETH,* *Worcester Polytechnic Institute, Worcester, Mass. and Palmer Physical Laboratory, Princeton University*

(Received May 8, 1936)

The electromagnetic theory of the torque exerted by a beam of polarized light on a doubly refracting plate which alters its state of polarization is summarized. The same quantitative result is obtained by assigning an angular momentum of $\hbar$ $(-\hbar)$ to each quantum of left (right) circularly polarized light in a vacuum, and assuming the conservation of angular momentum holds at the face of the plate. The apparatus used to detect and measure this effect was designed to enhance the moment of force to be measured by an appropriate arrangement of quartz wave plates, and to reduce interferences. The results of about 120 determinations by two observers working independently show the magnitude and sign of the effect to be correct, and show that it varies as predicted by the theory with each of three experimental variables which could be independently adjusted.

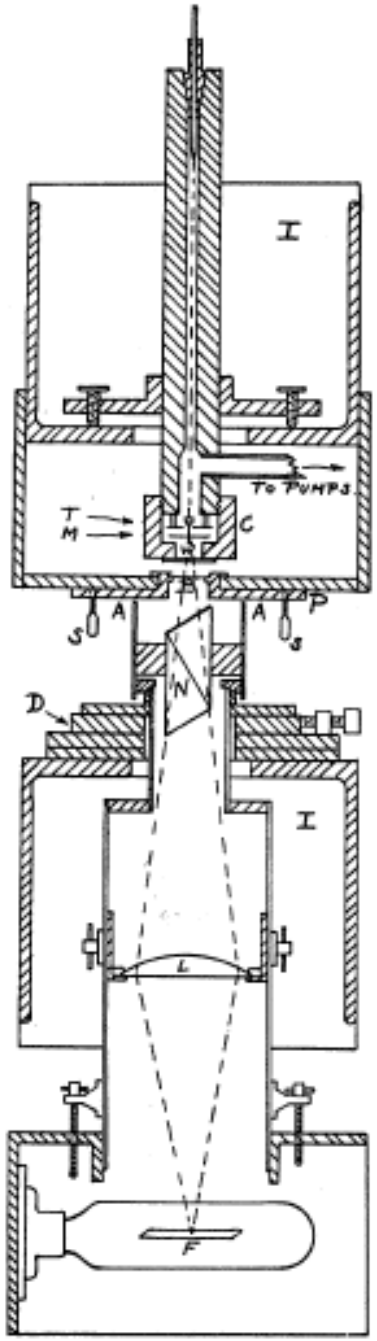

FIG. 1. Diagram of apparatus.

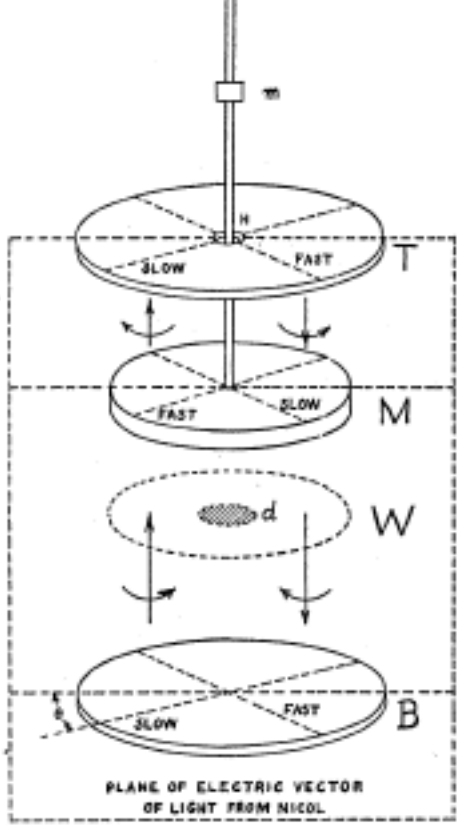

FIG. 3. Wave plate arrangement.

Besides almost quadrupling the torque compared to what would be obtained if the light were simply absorbed, and furthermore reducing heating, radiometer, and gas effects in the vacuum chamber, this plate arrangement greatly reduced difficulties due to radiation pressure. The disk M cannot be mounted exactly at right angles to the fiber axis, nor can the light be projected exactly in a vertical direction. Thus the resultant light pressure integrated over the disk will not be quite vertical and will produce a "light pressure torque" unless its line of action lies in a vertical plane containing the fiber axis. Without special precautions this torque might very easily mask the effect to be detected and measured.[10]

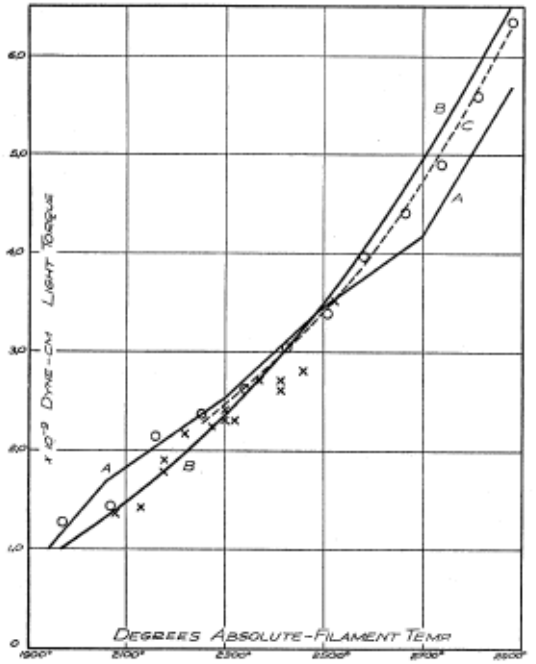

FIG. 6. Comparison of theory and experiment. Type I measurements: light torque as a function of filament temperature.

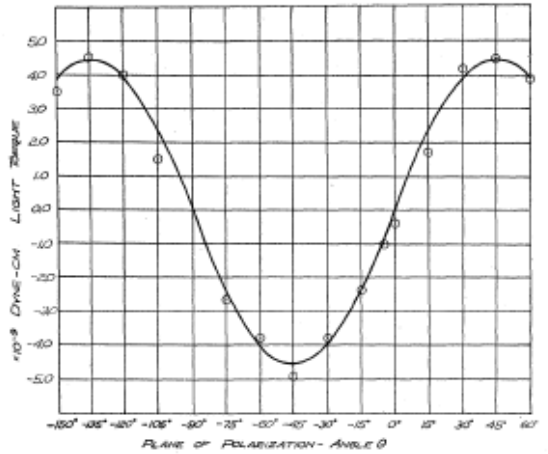

FIG. 8. Type II measurements: variation of light torque with angle between plane of polarization of light and the axes of the plates.

Photon *Orbital* Angular Momentum

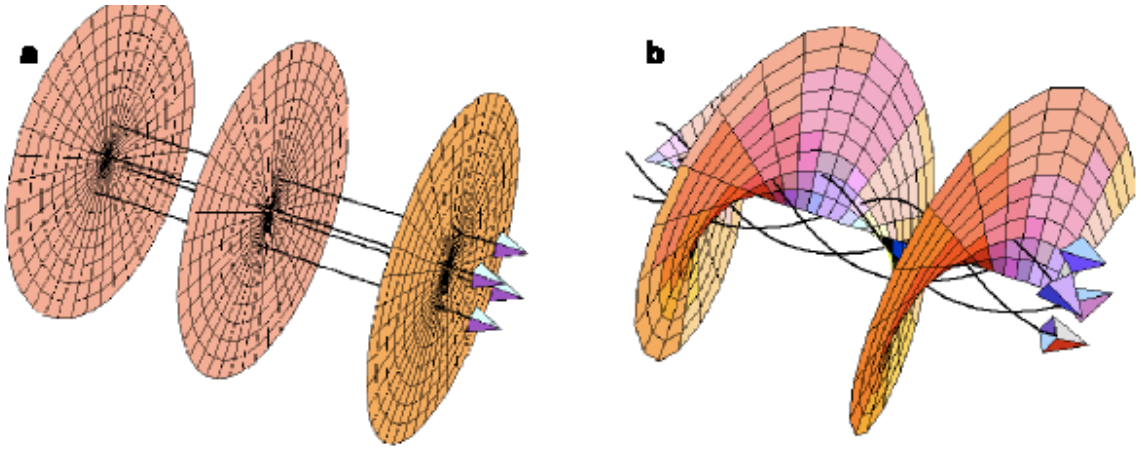

Figure 1. Laser beams usually have planar wavefronts with wavevectors parallel to the beam axis. Beams with helical wavefronts have wavevectors which spiral around the beam axis and give rise to an orbital angular momentum.

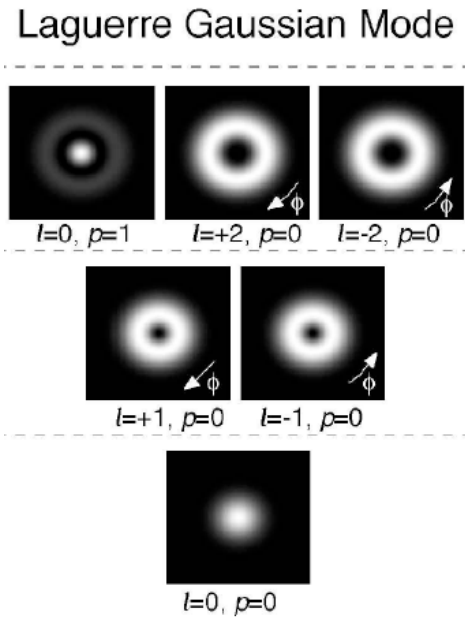

VOLUME 88, NUMBER 25 PHYSICAL REVIEW LETTERS 24 JUNE 2002

Measuring the Orbital Angular Momentum of a Single Photon

Jonathan Leach,[1] Miles J. Padgett,[1] Stephen M. Barnett,[2] Sonja Franke-Arnold,[2] and Johannes Courtial[1,*]

[1]*Department of Physics and Astronomy, University of Glasgow, Glasgow, Scotland*
[2]*Department of Physics and Applied Physics, University of Strathclyde, Glasgow, Scotland*
(Received 21 January 2002; published 5 June 2002)

We propose an interferometric method for measuring the orbital angular momentum of single photons. We demonstrate its viability by sorting four different orbital angular momentum states, and are thus able to encode two bits of information on a single photon. This new approach has implications for entanglement experiments, quantum cryptography and high density information transfer.

http://www.physics.gla.ac.uk/Optics/play/photonOAM/

“Orbital” Angular Momentum of Photons

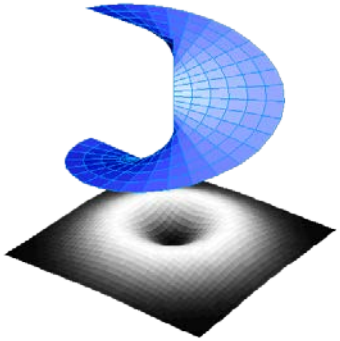

- Donut modes- Laguerre-Gaussian
- Phase SINGULARITY
- Quantized in multiples of $\hbar$

$|-1\rangle$ = L

$|0\rangle$ = G

$|1\rangle$ = R

Qutrits!

Holographic Preparation/Detection

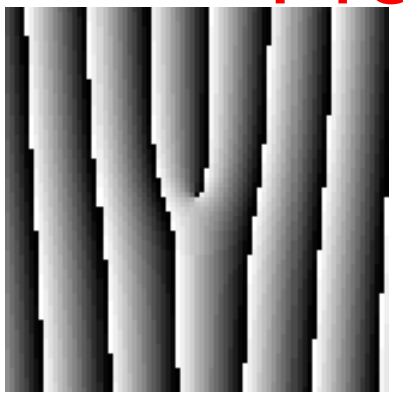

Diffraction at a dislocation changes the donut mode angular momentum

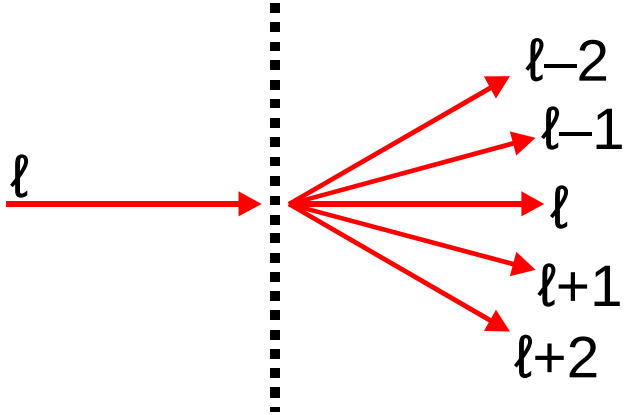

- Couple into single-mode fiber -- only accepts Gaussian mode; all others too big and cannot propagate inside fiber
- Together with the hologram we can detect other spatial modes

Efficient Sorting of Orbital Angular Momentum States of Light

Gregorius C. G. Berkhout,[1,2,*] Martin P. J. Lavery,[3,†] Johannes Courtial,[3] Marco W. Beijersbergen,[1,2] and Miles J. Padgett[3]

We present a method to efficiently sort orbital angular momentum (OAM) states of light using two static optical elements. The optical elements perform a Cartesian to log-polar coordinate transformation, converting the helically phased light beam corresponding to OAM states into a beam with a transverse phase gradient. A subsequent lens then focuses each input OAM state to a different lateral position. We demonstrate the concept experimentally by using two spatial light modulators to create the desired optical elements, applying it to the separation of eleven OAM states.

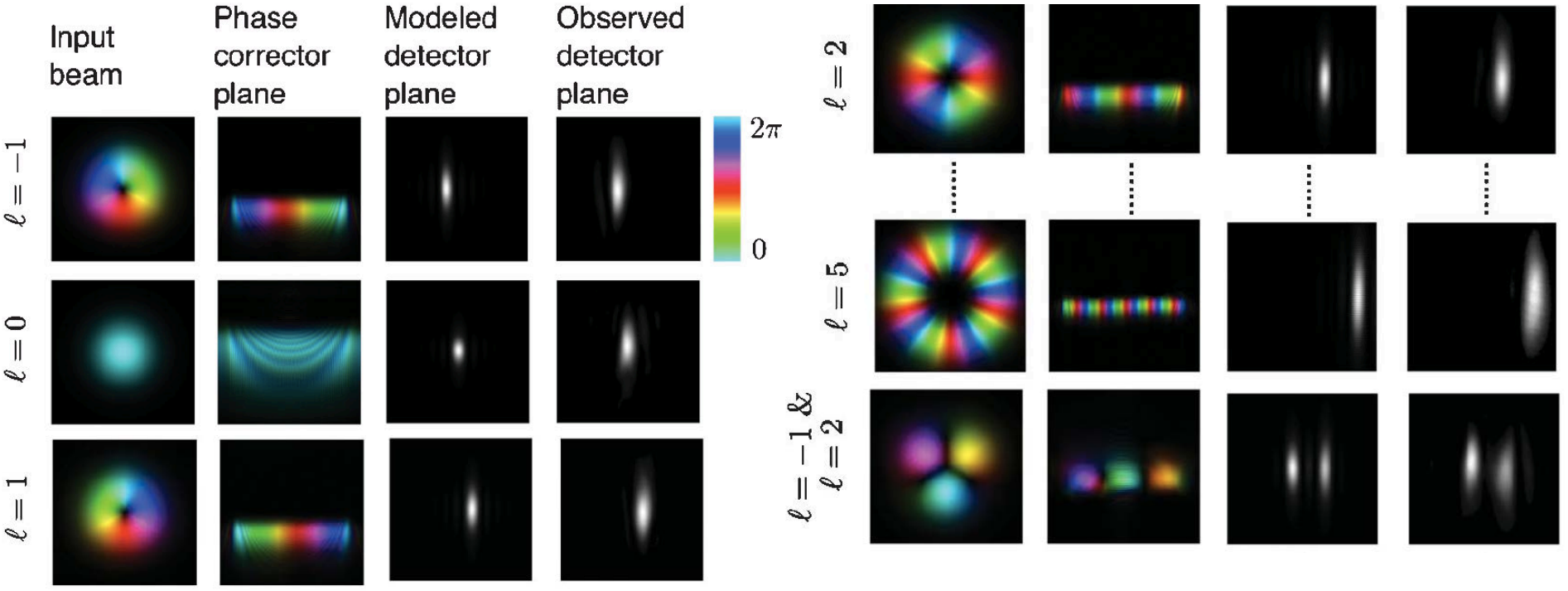

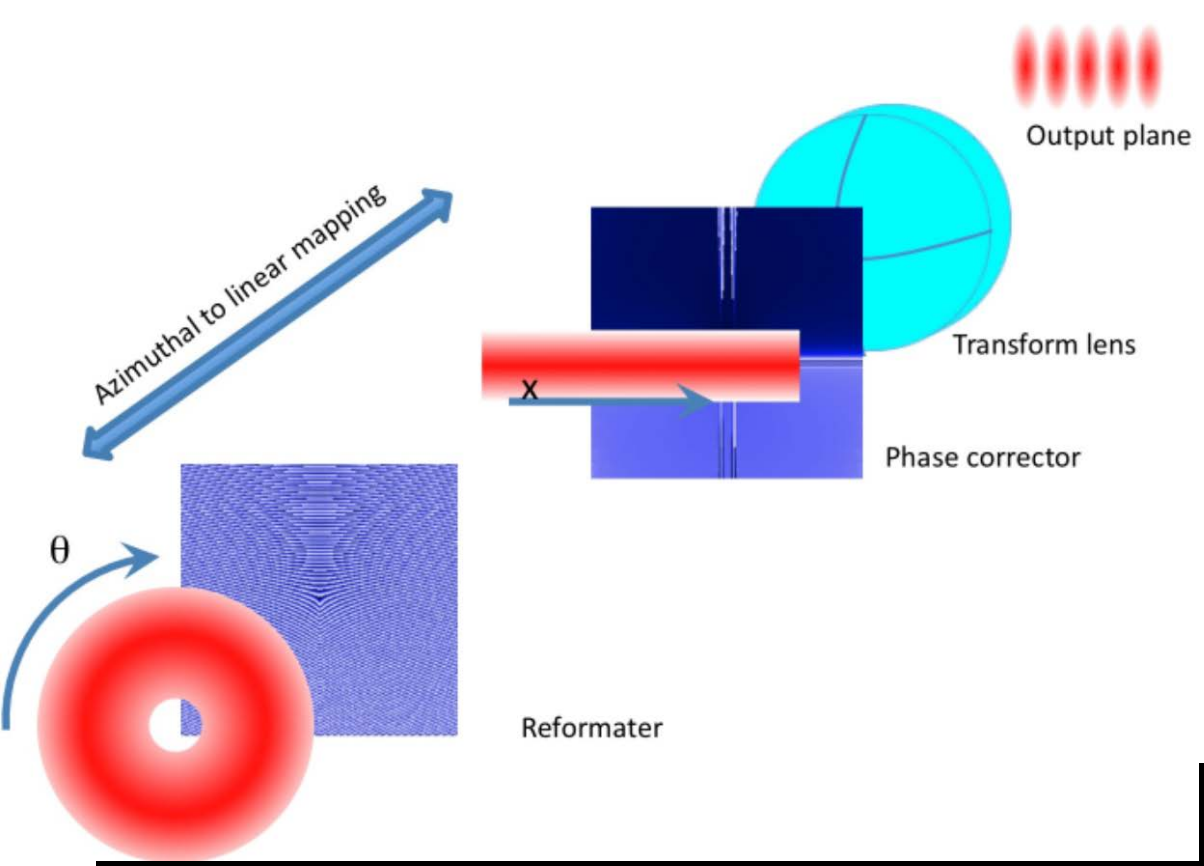

AOM Mode Sorter

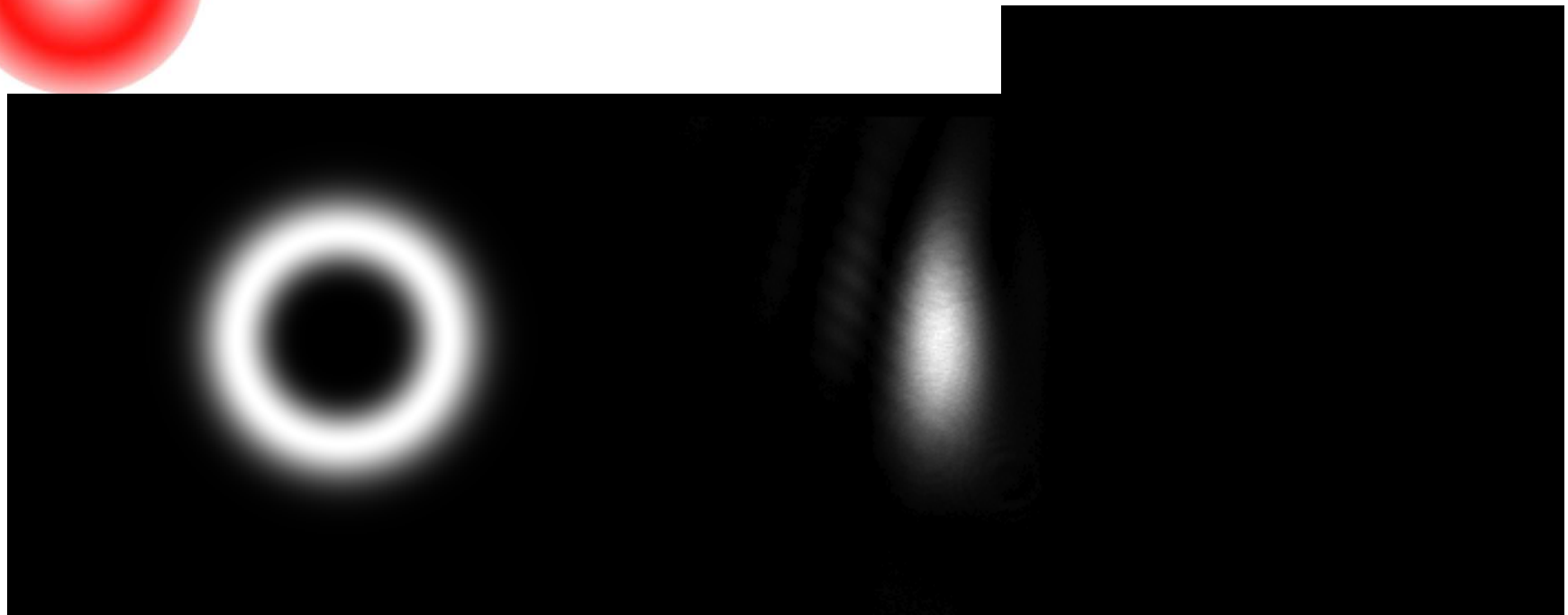

100 Tbit/s free-space data link enabled by three-dimensional multiplexing of orbital angular momentum, polarization, and wavelength

Hao Huang,[1,*] Guodong Xie,[1] Yan Yan,[1] Nisar Ahmed,[1] Yongxiong Ren,[1] Yang Yue,[1] Dvora Rogawski,[1] Moshe J. Willner,[1] Baris I. Erkmen,[2] Kevin M. Birnbaum,[2] Samuel J. Dolinar,[2] Martin P. J. Lavery,[3] Miles J. Padgett,[3] Moshe Tur,[4] and Alan E. Willner[1]

We investigate the orthogonality of orbital angular momentum (OAM) with other multiplexing domains and present a free-space data link that uniquely combines OAM-, polarization-, and wavelength-division multiplexing. Specifically, we demonstrate the multiplexing/demultiplexing of 1008 data channels carried on 12 OAM beams, 2 polarizations, and 42 wavelengths. Each channel is encoded with 100 Gbit/s quadrature phase-shift keying data, providing an aggregate capacity of 100.8 Tbit/s (12 × 2 × 42 × 100 Gbit/s).

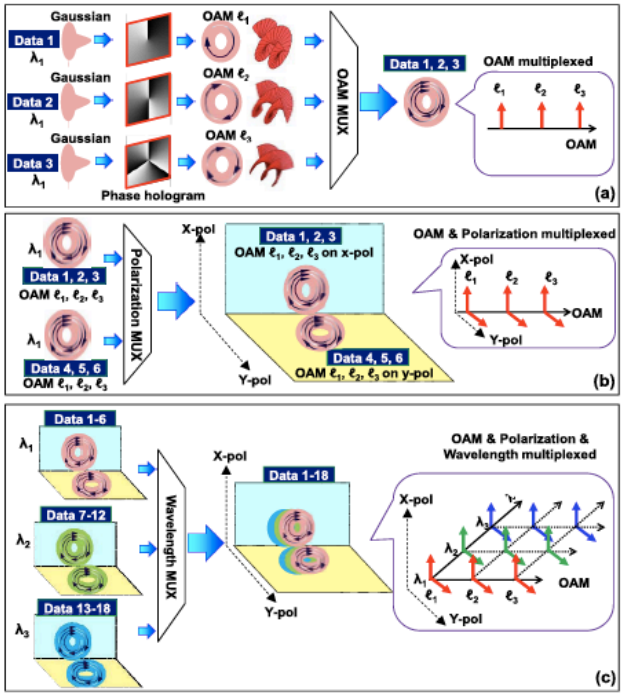

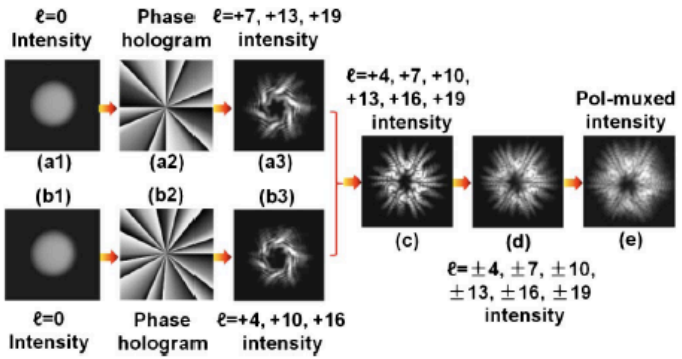

Fig. 3. Designed holograms and images of multiplexed OAM beams. (a1) Gaussian beam. (a2) Phase hologram for generating three OAM beams ($\ell = +4, +10$, and $+16$). (a3) Generated OAM beam including $\ell = +4, +10$, and $+16$. (b1) Gaussian beam. (b2) Phase hologram for generating three OAM beams ($\ell = +7, +13$, and $+19$). (b3) Generated OAM beams ($\ell = +7, +13$, and $+19$). (c) Multiplexed OAM beams with $\ell = +4, +7, +10, +13, +16$, and $+19$. (d) Multiplexed OAM beams with $\ell = \pm 4, \pm 7, \pm 10, \pm 13, \pm 16$, and ± 19. (e) Polarization-multiplexed OAM beams including $\ell = \pm 4, \pm 7, \pm 10, \pm 13, \pm 16$, and ± 19 on both x and y polarization.

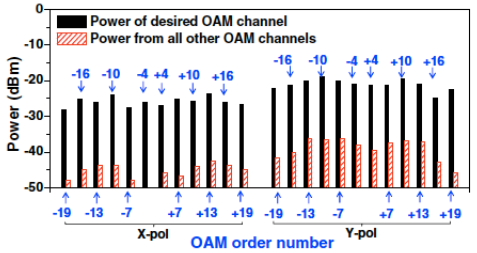

Fig. 4. Crosstalk measurement for all the OAM beams at a single wavelength (1552.26 nm).

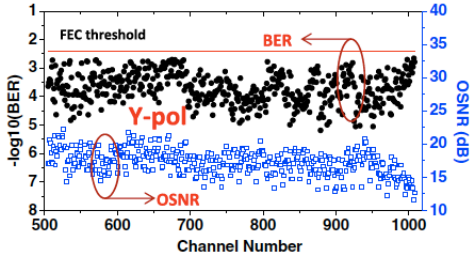

Fig. 7. Measured BER and OSNR for all 1008 channels (504 channels in x-pol and 504 channels in y-pol.).

Synopsis: Entangled Quadruplet

February 16, 2016

Four photons are shown to be entangled through their orbital angular momentum.

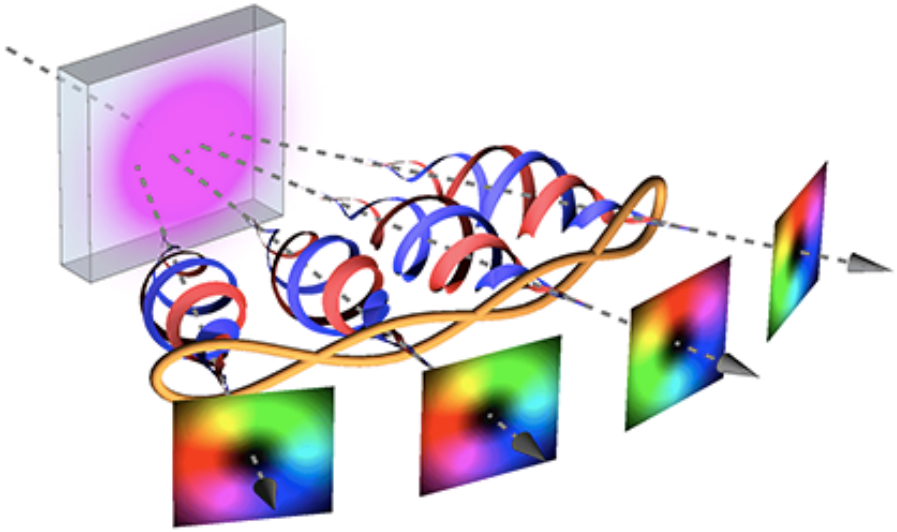

W. Löffler/Leiden University

Observation of Four-Photon Orbital Angular Momentum Entanglement
B. C. Hiesmayr, M. J. A. de Dood, and W. Löffler
Phys. Rev. Lett. 116, 073601 (2016)
Published February 16, 2016